

**Politecnico di Milano**

**Prova finale: Introduzione all'analisi di missioni spaziali**

AA 2023-2024

**Docente:**

Massari Mauro

# **Elaborato n. C12**

**Autori:**

10765584 Pirola Ilaria

10800138 Piscaglia Mattia

10766305 Riboni Gabriele

Data di consegna: 23/11/2023

# Table of contents

<b>1</b>	<b>Introduction</b>	<b>3</b>
<b>2</b>	<b>Initial orbit characterisation</b>	<b>3</b>
2.1	Description of the initial parameters . . . . .	3
2.2	Description of the initial orbit . . . . .	3
2.3	Graphical representation of the initial orbit . . . . .	4
<b>3</b>	<b>Final orbit characterisation</b>	<b>4</b>
3.1	Description of the final parameters . . . . .	4
3.2	Description of the final orbit . . . . .	4
3.3	Graphical representation of the final orbit . . . . .	5
<b>4</b>	<b>Transfer trajectory: definition and analysis</b>	<b>5</b>
4.1	Introduction to the developed strategies . . . . .	5
4.2	Possible transfer strategies . . . . .	5
4.2.1	Standard strategy . . . . .	5
4.2.2	First alternative strategy: <i>bi-elliptic transfer</i> . . . . .	7
4.2.3	Second alternative strategy: <i>circularisation and Hohmann transfer</i> . . . . .	7
4.2.4	Third alternative strategy: <i>Tangent transfer followed by a secant intersection to the final orbit</i> . . . . .	8
4.2.5	Fourth alternative strategy: <i>direct transfer</i> . . . . .	9
<b>5</b>	<b>Conclusions</b>	<b>10</b>
<b>6</b>	<b>Appendix</b>	<b>11</b>

# 1 Introduction

The following report aims to describe the transfer of a satellite from a starting point on an initial orbit to an ending point on a final orbit.

Several strategies are studied, trying to optimise the total fuel consumption (i.e. the economic cost) or/and the duration of the transfer.

All the maneuvers described, from the assigned standard strategy to the most significant alternatives, were implemented and developed using Matlab®.

The value of the gravitational parameter used in the calculations is  $\mu = 398600 \frac{km^3}{s^2}$ .

The work was divided equally among all group members, in both developing the strategies and producing the report and the presentation.

The following report contains few significant figures, specific data are available in the appendix.

## 2 Initial orbit characterisation

### 2.1 Description of the initial parameters

Given position and velocity on the initial orbit, expressed in the Geocentric Equatorial Inertial System, Keplerian parameters were calculated in a perifocal coordinate system using car2par function.

$r_x$ [km]	$r_y$ [km]	$r_z$ [km]	$v_x$ [km/s]	$v_y$ [km/s]	$v_z$ [km/s]
4643.9563	5721.0035	2608.9369	-5.6160	2.6040	4.2930

Table 1: Initial point in the GEI system

a [km]	e [-]	i [rad]	$\Omega$ [rad]	$\omega$ [rad]	$\theta$ [rad]
8811.7585	0.1129	0.7213	0.4745	0.5270	0.0029

Table 2: Keplerian parameters

### 2.2 Description of the initial orbit

The shape and the size of the initial orbit are characterized by a semi-major axis of 8811.7585 km and an eccentricity of 0.1129.

Looking at these data, it is possible to see that the orbit is almost circular, and this is confirmed by the calculation of the semi-latus rectum,  $p = 8699.4202$  km.

The orbital plane has an inclination of  $41.3252^\circ$  from the Z axis of the GEI System, a longitude of the ascending node of  $27.1877^\circ$  and a periapsis argument of  $30.1957^\circ$ . The true anomaly of the starting point is  $0.1650^\circ$ .

Other considerable data for the following analyses are the perigee and apogee radii,  $r_p = 7816.8223$  km and  $r_a = 9806.6947$  km, the orbital period,  $T = 8231.9951$  s, and the specific mechanical energy,  $E = -22.6175 \frac{km^2}{s^2}$ .

## 2.3 Graphical representation of the initial orbit

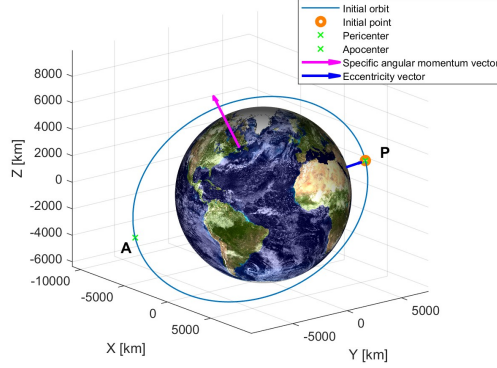


Figure 1

## 3 Final orbit characterisation

### 3.1 Description of the final parameters

Given the Keplerian parameters of the final orbit in a perifocal coordinate system, position and velocity in the Geocentric Equatorial Inertial were founded using par2car function.

a [km]	e [-]	i [rad]	$\Omega$ [rad]	$\omega$ [rad]	$\theta$ [rad]
14160.0	0.2088	1.4870	1.6100	2.3450	1.5110

Table 3: Keplerian parameters

$r_x$ [km]	$r_y$ [km]	$r_z$ [km]	$v_x$ [km/s]	$v_y$ [km/s]	$v_z$ [km/s]
1128.9745	-10068.6270	-8732.6425	0.3015	2.7585	-4.8735

Table 4: Final point in the GEI system

### 3.2 Description of the final orbit

The final orbit has a semi-major axis of 14160.0 km and an eccentricity of 0.2088, consequently it is more elliptical than the first orbit and larger in size.

The orbital plane is inclined of  $85.1988^\circ$  from the Z axis of the GEI System.

The right ascension of the ascending node is  $92.2462^\circ$ , the argument of periapsis is  $134.3586^\circ$  and the true anomaly of the final point is  $86.5739^\circ$ .

The other remarkable values are the semi-latus rectum,  $p = 13542.6602$  km, perigee and apogee radii,  $r_p = 11203.3920$  km and  $r_a = 17116.6080$  km, the orbital period,  $T = 16768.9589$  s, and the specific mechanical energy,  $E = -14.0749 \frac{\text{km}^2}{\text{s}^2}$ .

### 3.3 Graphical representation of the final orbit

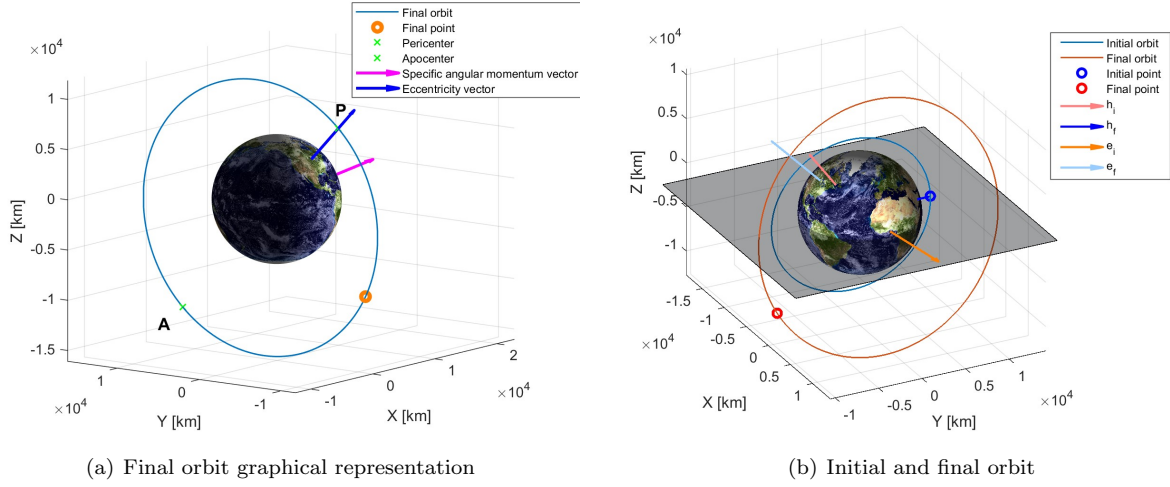


Figure 2

## 4 Transfer trajectory: definition and analysis

### 4.1 Introduction to the developed strategies

Different strategies are available to reach the final point. The standard strategy is developed to give an initial idea of costs and time. Then several alternatives are implemented to reduce the two values.

The following are being considered:

- A bi-elliptic transfer followed by a change of plane to optimise the  $\Delta v$  of the maneuver. Before completing the transfer a change of periapsis argument is performed.
- A bitangent transfer on a circular auxiliary orbit after having circularized the initial and the final orbit (Hohmann transfer), followed by a change of plane and periapsis argument and finally a change of shape is performed to achieve the final parameters.
- A tangent pulse after a change of plane followed by a secant transfer between the auxiliary orbit and the final one, changing also the periapsis argument.
- A direct strategy using a single transfer orbit secant to the initial one in the starting point  $\theta_i$  and to the second one in the final position  $\theta_f$ .

### 4.2 Possible transfer strategies

#### 4.2.1 Standard strategy

The target is to transfer the satellite from the initial orbit to the final one through a maneuver with three auxiliary orbits and four pulses. In order a change of plane, a change of pericenter anomaly and finally a change of shape are performed. (Figure 4)

In the following paragraph the three pulses are analysed:

- The first impulse is needed to bring the inclination of the orbit from the initial ( $i_i$ ) to the final one ( $i_f$ ) and the right ascension of the ascending node to his final value ( $\Omega_f$ ).

As a change of plane this maneuver causes also a change in the pericenter anomaly  $\omega$ .

- The pericenter anomaly must be changed again to achieve the correct alignment with that of the final one ( $\omega_f$ ).

To do so, a secant transfer is executed; the impulse can be given at two different intersections, one of these is better than the other one considering the costs in terms of impulse and time. The graphical representation and the following explanations will help understand this idea. (Figure 3)

- Finally, it is necessary to change the shape of the orbit (semi-major axis and eccentricity) through a bi-tangent maneuver from the pericenter of the departure orbit to the apocenter of the final one.

Obviously, this maneuver is the less expensive in terms of costs because in the pericenter the velocity of the satellite is the highest of the orbit so a lower  $\Delta v$  is necessary.

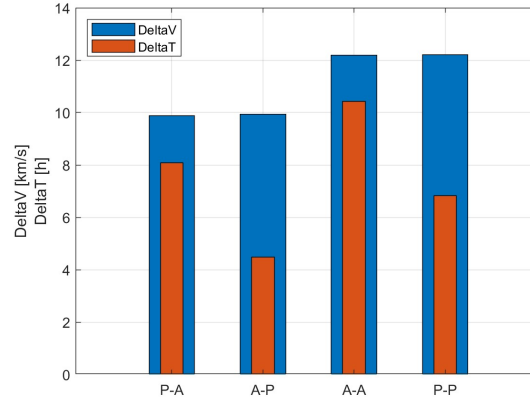


Figure 3: Bar chart showing the costs in terms of time and velocity in four different cases. The time is expressed in hours. (P = pericenter and A = apocenter)

The chart in *figure 3* has been obtained by combining all the possible bi-tangent maneuver from the auxiliary orbit to the final one.

Analysing the bar chart (Figure 1), it's easily understandable that the pericenter-apocenter bi-tangent transfer is the less expensive in terms of costs but not in terms of time ( $\Delta v = 9.8756 \frac{km}{s}$ ,  $\Delta t = 29110 s$ ).

To minimise the  $\Delta t$  with this type of strategy it's necessary to perform an apocenter-pericenter bi-tangent transfer ( $\Delta v = 9.9444 \frac{km}{s}$ ,  $\Delta t = 16147 s$ ).

Despite this, the standard strategy is not the most efficient in many aspects, so a number of alternative strategies have been studied.

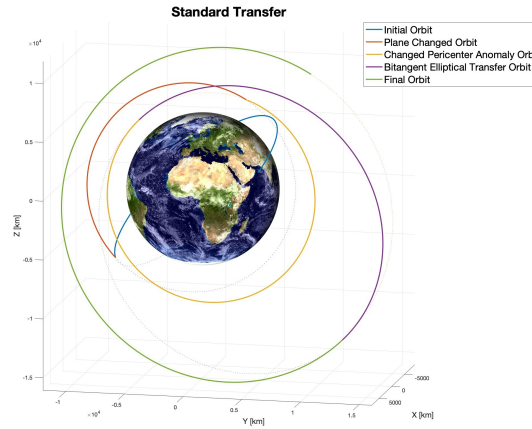


Figure 4: Standard transfer P-A

#### 4.2.2 First alternative strategy: *bi-elliptic transfer*

The first alternative strategy (Figure 5b) is performed to reduce the costs of the maneuver of changing plane in a more efficient point.

It consists of five pulses and four auxiliary orbits. In order, the five pulses are: bi-elliptical transfer starting from the pericenter (three pulses), change of plane and change of pericenter anomaly.

During this type of maneuver the  $\Delta v$  depends on the distance of the satellite from the Earth, so a bi-elliptical transfer could help because the satellite will be on an auxiliary orbit with an apocenter further than the initial one.

It is possible to use a for loop to have an idea on which is the best distance.

Naturally, the change of plane will be performed in a different point ( $\theta = 3.9049 \text{ rad}$ ) from the furthest one of the transfer orbit (apocenter,  $\theta_a = \pi$ ). To execute the plane change in the last one of the auxiliary orbit it is necessary to change the pericenter anomaly before changing plane and then change it again.

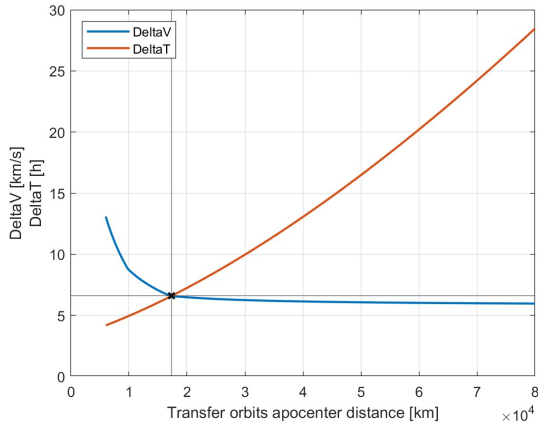
It is known that changing pericenter anomaly before changing plane is useless and not really correct.

Consequently, it has been decided to change only one time the  $\omega$  after being on an orbit with the same shape of the final one but with a different pericenter argument.

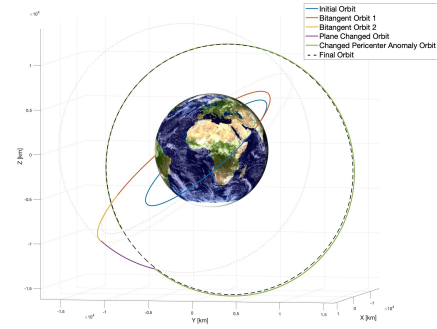
Showing the  $\Delta v$  and  $\Delta t$ , before the change of pericenter anomaly, as a function of the transfer orbits' apocenter radius, it is possible to choose a convenient value of  $r_a$  for both parameters: time and velocity. (Figure 5a)

In fact, using the intersection point between the two graphs, the  $\Delta v$  is quite similar to the asymptotic value and the time is reasonable.

Naturally the total  $\Delta v$  and  $\Delta t$  are calculated considering also the last maneuver performed to change the pericenter anomaly. ( $\Delta v = 8.7061 \frac{km}{s}$ ,  $\Delta t = 52066 \text{ s}$ )



(a) Bi-elliptic with change of plane



(b) First alternative

Figure 5

#### 4.2.3 Second alternative strategy: *circularisation and Hohmann transfer*

This strategy is performed to evaluate the convenience of the Hohmann transfer.

It consists of five pulses and six auxiliary orbits. (Figure 6)

First the initial orbit is circularised ( $e = 0$ ) using the apocenter radius.

Then an Hohmann transfer is executed and in the meantime, while the satellite is on the auxiliary orbit with the same semi-axis of the final one, a change of plane and pericenter argument is performed.

Finally, the Hohmann transfer is concluded to reach another auxiliary orbit with the same parameters of the final ones except for the eccentricity.

Then, using the last maneuver from the pericenter the satellite could reach the final orbit with the correct eccentricity.

This type of maneuver has an lower cost in terms of  $\Delta v$  rather than the bi-elliptic strategy and a lower time also ( $\Delta v = 7.9673 \frac{km}{s}$ ,  $\Delta t = 36617 \text{ s}$ ).

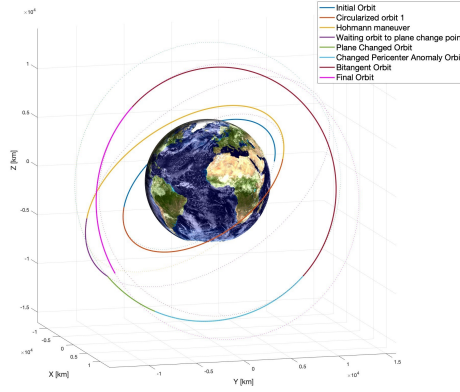


Figure 6: Second alternative

#### 4.2.4 Third alternative strategy: *Tangent transfer followed by a secant intersection to the final orbit*

The third alternative strategy consists of two auxiliary orbits and three pulses. (Figure 7)

As the standard strategy, the first is a change of plane, then a tangent pulse is executed starting from the initial point to achieve an auxiliary orbit secant to the final one. The last pulse bring the satellite from the transfer orbit to the last one changing also the pericenter anomaly.

Using a for loop, a large number of orbits characterised by a different intersection with the final orbit were considered.

In particular, two of them are significant. In fact trying to minimise the  $\Delta v$  and  $\Delta t$  it is possible to identify the following results:

- Minimisation of  $\Delta v$ :  $\Delta v = 8.5063 \frac{km}{s}$ ,  $\Delta t = 16992 s$
- Minimisation of  $\Delta t$ :  $\Delta v = 8.8634 \frac{km}{s}$ ,  $\Delta t = 14444 s$

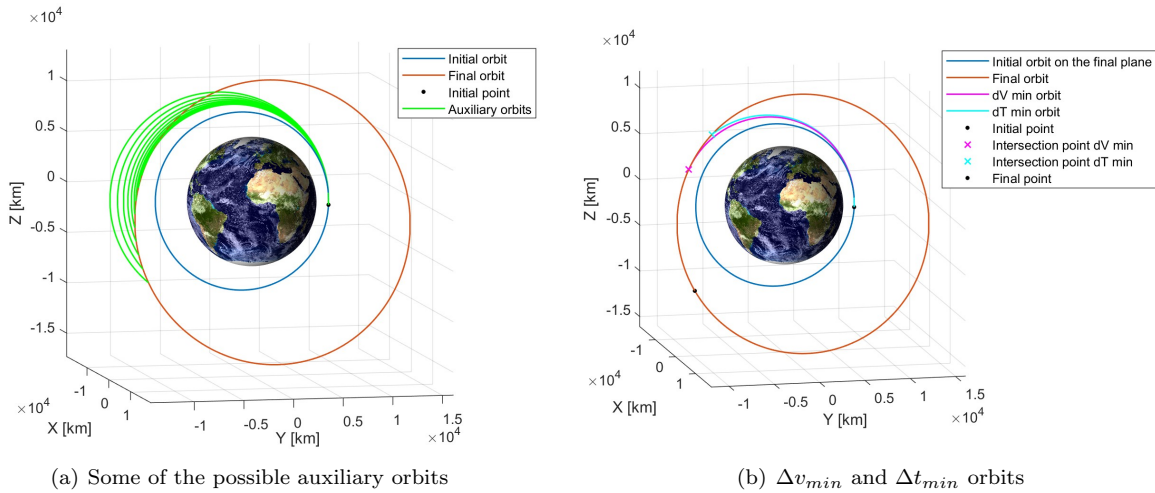


Figure 7



#### 4.2.5 Fourth alternative strategy: *direct transfer*

The fourth alternative strategy consists of two pulses and only one auxiliary orbit. (Figure 8)

This orbit is secant to the first one in the initial point ( $\theta_i$ ) and to the second one in the final point ( $\theta_f$ ).

Its characterisation is obtained by imposing the direction of the orbital angular momentum as a vector product of the initial and the final radii.

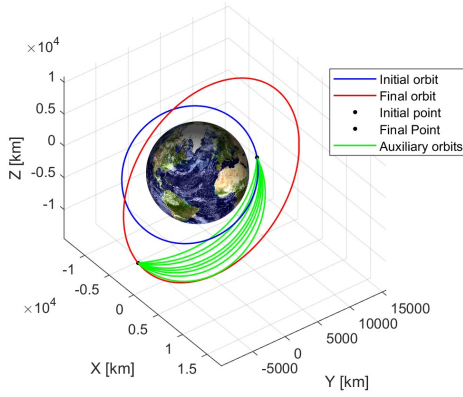
It is notable that this result is not the actual value of the orbital angular momentum, nevertheless it is used to identify the inclination ( $i_t$ ) of the auxiliary orbit. Same thing for the nodal axis (N), as only the versor is necessary to calculate the right ascension of the ascending node  $\Omega_t$ .

To find the difference between the two thetas of the transfer orbit, it is possible to use the inverse of the scalar product between the two radii ( $r_i$  and  $r_f$ ).

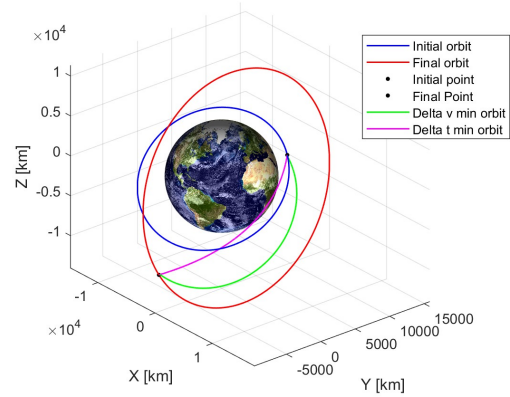
Then, using a for loop all the possible orbits are plotted and with some conditions on eccentricity ( $0 < e < 1$ ) and pericenter (pericenter radius greater than Earth radius plus one hundred kilometers,  $r_p > R_{earth} + 100km$ ) only a number of them are available.

Among all of them, the most significant ones are those that minimise the  $\Delta v$  and  $\Delta t$ :

- Minimisation of  $\Delta v$ :  $\Delta v = 23.8082 \frac{km}{s}$ ,  $\Delta t = 2200 s$
- Minimisation of  $\Delta t$ :  $\Delta v = 27.1790 \frac{km}{s}$ ,  $\Delta t = 5150 s$



(a) Some of the possible auxiliary orbits



(b)  $\Delta v_{min}$  and  $\Delta t_{min}$  orbits

Figure 8

## 5 Conclusions

In conclusion, it could be interesting to compare the results obtained by implementing the various strategies. The parameters to minimise are time and cost.

Analysing the bar chart in *figure 9a*, it is noticeable that the cost ( $\Delta v$ ) of the second alternative is the cheapest as expected from theory. Nevertheless, in terms of time this strategy is even less convenient than the standard one.

To minimise the time, the fourth alternative with  $\Delta t_{min}$  turns out to be the most advantageous but with a really excessive cost compared to other alternatives.

The graph in *figure 9b* could be useful to find the best solution considering both time and  $\Delta v$ . The fourth alternative with minimum  $\Delta t$ , considering the product of time and cost as a comparison parameter, is the most convenient. In fact, it is observed that the equilateral hyperbola related to this strategy is the lowest among the others. (Figure 9b)

However, the standard strategy, excluding the two direct transfers, represents the best trade-off between time and fuel consumption among all the “cheapest” strategies.

Anyway, in choosing which strategy to use, the minimisation of  $\Delta v$  is more important than the minimisation of transfer time.

The reason comes from the direct link between the impulse  $\Delta v$  and the propellant mass carried by the spacecraft, obtainable by the Tsiolkovsky’s equation:

$$m_p = m_0 * (1 - e^{\frac{-\Delta v}{g_0 * I_s}})$$

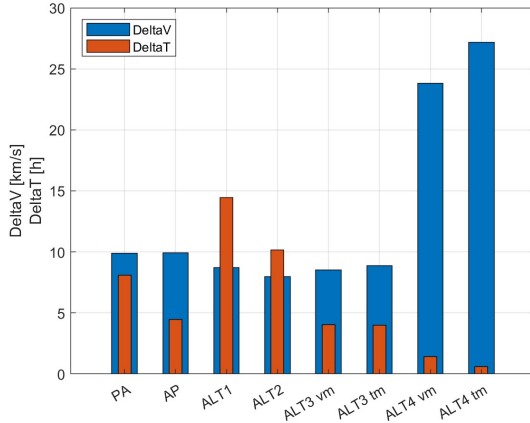
$m_p$ : propellant mass;

$m_0$ : initial total mass;

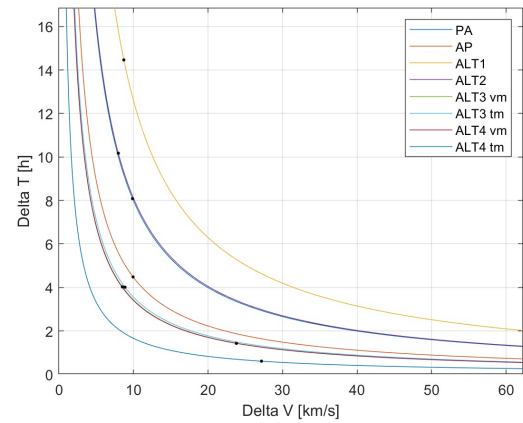
$\Delta v$ : impulse of velocity;

$g_0$ : standard acceleration due to gravity;

$I_s$ : specific impulse.



(a) Bar chart



(b) Graph

Figure 9

## 6 Appendix

Bold numbers indicate the total of time and impulses for each strategy.

t [s]	a [km]	e [-]	i [rad]	$\Omega$ [rad]	$\omega$ [rad]	$\theta$ [rad]	$\Delta v$ [km/s]
0	8811.7585	0.1129	0.7213	0.4745	0.5270	0.0029	-
5330.5965	8811.7585	0.1129	0.7213	0.4745	0.5270	3.9049	7.1407
	8811.7585	0.1129	1.4870	1.6100	-0.0730	3.9049	
9544.8619	8811.7585	0.1129	1.4870	1.6100	-0.0730	1.2090	1.4296
	8811.7585	0.1129	1.4870	1.6100	2.3450	5.0742	
10860.7163	8811.7585	0.1129	1.4870	1.6100	2.3450	0	0.8340
	12466.7152	0.3730	1.4870	1.6100	2.3450	0	
17787.1436	12466.7152	0.3730	1.4870	1.6100	2.3450	$\pi$	0.4713
	14160	0.2088	1.4870	1.6100	2.3450	$\pi$	
<b>29110.0717</b>	14160	0.2088	1.4870	1.6100	2.3450	1.5110	-
-	-	-	-	-	-	-	<b>9.8756</b>

Table 5: Standard strategy P-A

t [s]	a [km]	e [-]	i [rad]	$\Omega$ [rad]	$\omega$ [rad]	$\theta$ [rad]	$\Delta v$ [km/s]
0	8811.7585	0.1129	0.7213	0.4745	0.5270	0.0029	-
5330.5965	8811.7585	0.1129	0.7213	0.4745	0.5270	3.9049	7.1407
	8811.7585	0.1129	1.4870	1.6100	-0.0730	3.9049	
5981.6900	8811.7585	0.1129	1.4870	1.6100	-0.0730	4.3506	1.4296
	8811.7585	0.1129	1.4870	1.6100	2.3450	1.9326	
7850.3700	8811.7585	0.1129	1.4870	1.6100	2.3450	$\pi$	0.5792
	10505.0433	0.0665	1.4870	1.6100	2.3450	$\pi$	
13208.0651	10505.0433	0.0665	1.4870	1.6100	2.3450	0	0.7949
	14160	0.2088	1.4870	1.6100	2.3450	0	
<b>16146.5137</b>	14160	0.2088	1.4870	1.6100	2.3450	1.5110	-
-	-	-	-	-	-	-	<b>9.9444</b>

Table 6: Standard strategy A-P

t [s]	a [km]	e [-]	i [rad]	$\Omega$ [rad]	$\omega$ [rad]	$\theta$ [rad]	$\Delta v$ [km/s]
0	8811.7585	0.1129	0.7213	0.4745	0.5270	0.0029	-
8229.0076	8811.7585	0.1129	0.7213	0.4745	0.5270	0	0.8494
	12567.5612	0.3780	0.7213	0.4745	0.5270	0	
15239.6487	12567.5612	0.3780	0.7213	0.4745	0.5270	$\pi$	0.4686
	14260.8460	0.2144	0.7213	0.4745	0.5270	$\pi$	
18198.5752	14260.8460	0.2144	0.7213	0.4745	0.5270	3.9049	5.2540
	14260.8460	0.2144	1.4870	1.6100	-0.0730	3.9049	
23713.8575	14260.8460	0.2144	1.4870	1.6100	-0.0730	0	0.0152
	14160.0	0.2088	1.4870	1.6100	-0.0730	0	
36420.9058	14160	0.2088	1.4870	1.6100	-0.0730	4.3506	2.1189
	14160	0.2088	1.4870	1.6100	2.3450	1.9326	
<b>52066.4027</b>	14160	0.2088	1.4870	1.6100	2.3450	1.5110	
-	-	-	-	-	-	-	<b>8.7061</b>

Table 7: First alternative strategy

t [s]	a [km]	e [-]	i [rad]	$\Omega$ [rad]	$\omega$ [rad]	$\theta$ [rad]	$\Delta v$ [km/s]
0	8811.7585	0.1129	0.7213	0.4745	0.5270	0.0029	-
4113.01005	8811.7585	0.1129	0.7213	0.4745	0.5270	$\pi$	0.3707
	9806.6947	0	0.7213	0.4745	0.5270	$\pi$	
8945.4360	9806.6947	0	0.7213	0.4745	0.5270	0	0
	9806.6947	0	0.7213	0.4745	0.5270	0	
8945.4360	9806.6947	0	0.7213	0.4745	0.5270	0	0.8136
	13461.6513	0.2715	0.7213	0.4745	0.5270	0	
16717.3633	13461.6513	0.2715	0.7213	0.4745	0.5270	$\pi$	0.7069
	17116.6080	0	0.7213	0.4745	0.5270	$\pi$	
19424.7425	17116.6080	0	0.7213	0.4745	0.5270	3.9049	5.5429
	17116.6080	0	1.4870	1.6100	-0.0730	3.9049	
21005.6593	17116.6080	0	1.4870	1.6100	-0.0730	4.3506	0
	17116.6080	0	1.4870	1.6100	2.3450	1.9326	
25293.9553	17116.6080	0	1.4870	1.6100	2.3450	$\pi$	0.5333
	14160	0.2088	1.4870	1.6100	2.3450	$\pi$	
<b>36616.8834</b>	14160	0.2088	1.4870	1.6100	2.3450	1.5110	-
-	-	-	-	-	-	-	<b>7.9673</b>

Table 8: Second alternative strategy

t [s]	a [km]	e [-]	i [rad]	$\Omega$ [rad]	$\omega$ [rad]	$\theta$ [rad]	$\Delta v$ [km/s]
0	8811.7585	0.1129	0.7213	0.4745	0.5270	0.0029	-
5330.5965	8811.7585	0.1129	0.7213	0.4745	0.5270	3.9049	7.1407
	8811.7585	0.1129	1.4870	1.6100	-0.0730	3.9049	
8229.0076	8811.7585	0.1129	1.4870	1.6100	-0.0730	0	0.2583
	9656.9287	0.1905	1.4870	1.6100	-0.0730	0	
12254.5568	9656.9287	0.1905	1.4870	1.6100	-0.0730	2.8180	1.1072
	14160	0.2088	1.4870	1.6100	2.3450	0.4000	
<b>16991.9979</b>	14160.0	0.2088	1.4870	1.6100	2.3450	1.5110	-
-	-	-	-	-	-	-	<b>8.5063</b>

Table 9: Third alternative strategy with  $\Delta v_{min}$

t [s]	a [km]	e [-]	i [rad]	$\Omega$ [rad]	$\omega$ [rad]	$\theta$ [rad]	$\Delta v$ [km/s]
0	8811.7585	0.1129	0.7213	0.4745	0.5270	0.0029	-
5330.5965	8811.7585	0.1129	0.7213	0.4745	0.5270	3.9049	7.1407
	8811.7585	0.1129	1.4870	1.6100	-0.0730	3.9049	
8229.0076	8811.7585	0.1129	1.4870	1.6100	-0.0730	0	0.3181
	9880.6984	0.2089	1.4870	1.6100	-0.0730	0	
11505.3589	9880.6984	0.2089	1.4870	1.6100	-0.0730	2.4180	1.4046
	14160	0.2088	1.4870	1.6100	2.3450	0	
<b>14443.8075</b>	14160.0	0.2088	1.4870	1.6100	2.3450	1.5110	-
-	-	-	-	-	-	-	<b>8.8634</b>

Table 10: Third alternative strategy with  $\Delta t_{min}$

t [s]	a [km]	e [-]	i [rad]	$\Omega$ [rad]	$\omega$ [rad]	$\theta$ [rad]	$\Delta v$ [km/s]
0	8811.7585	0.1129	0.7213	0.4745	0.5270	0.0029	-
0	8811.7585	0.1129	0.7213	0.4745	0.5270	0.0029	15.3473
	10152.5610	0.3398	2.3920	3.6403	1.5445	5.2686	
5149.5967	10152.5610	0.3398	2.3920	3.6403	1.5445	2.3115	8.4609
	14160.0	0.2088	1.4870	1.6100	2.3450	1.5110	
<b>5149.5967</b>	14160.0	0.2088	1.4870	1.6100	2.3450	1.5110	-
-	-	-	-	-	-	-	<b>23.8082</b>

Table 11: Fourth alternative strategy with  $\Delta v_{min}$

t [s]	a [km]	e [-]	i [rad]	$\Omega$ [rad]	$\omega$ [rad]	$\theta$ [rad]	$\Delta v$ [km/s]
0	8811.7585	0.1129	0.7213	0.4745	0.5270	0.0029	-
0	8811.7585	0.1129	0.7213	0.4745	0.5270	0.0029	17.2303
	257887.5510	0.9741	2.3920	3.6403	3.4172	3.3958	
2199.6887	257887.5510	0.9741	2.3920	3.6403	3.4172	0.4388	9.9487
	14160.0	0.2088	1.4870	1.6100	2.3450	1.5110	
<b>2199.6887</b>	14160.0	0.2088	1.4870	1.6100	2.3450	1.5110	-
-	-	-	-	-	-	-	<b>27.1790</b>

Table 12: Fourth alternative strategy with  $\Delta t_{min}$